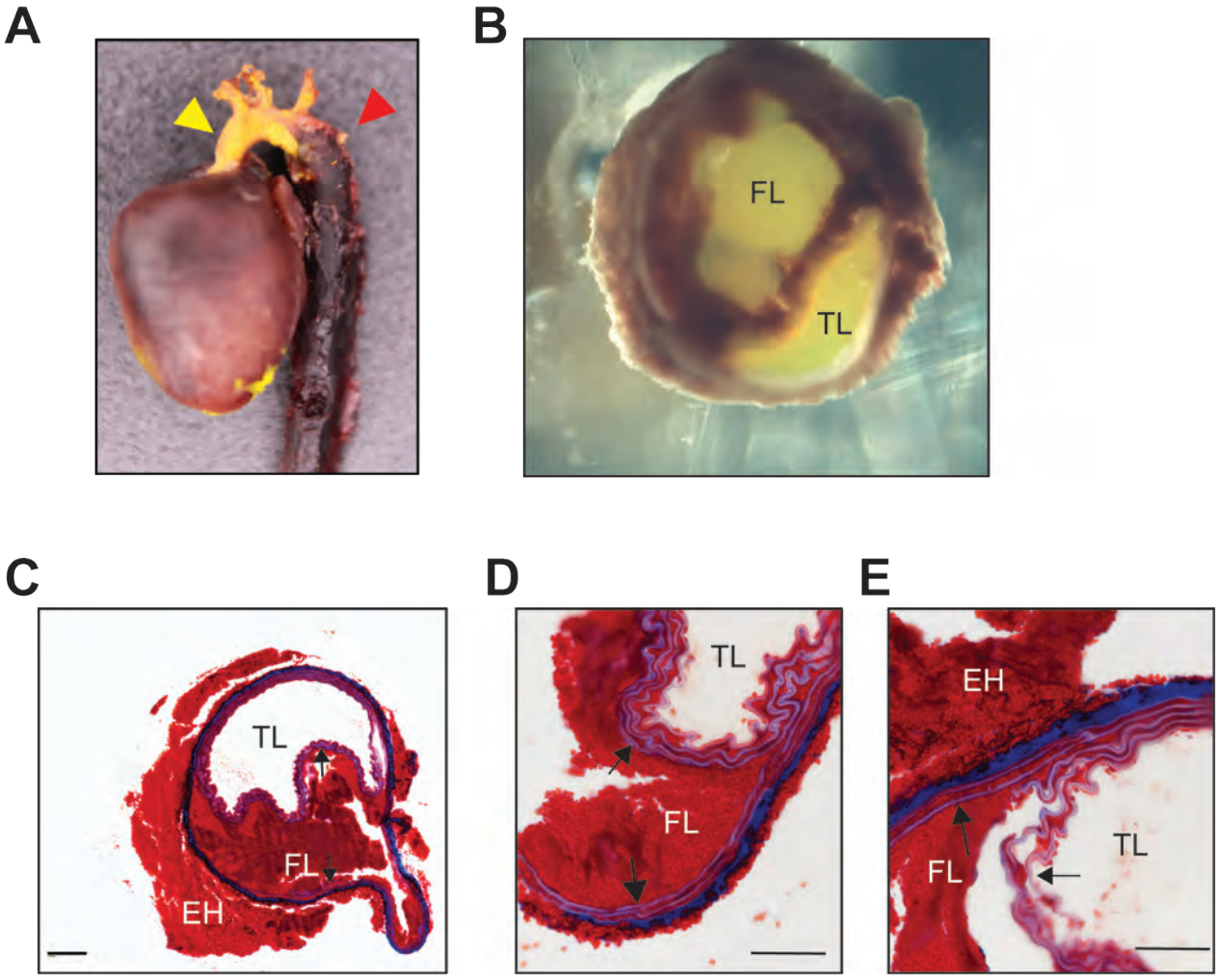

Supplementary Figure 1. vEDS mice develop spontaneous aortic rupture and dissection.
a, A representative gross post-mortem examination of a latex-injected aorta (yellow arrowhead) demonstrates descending aortic dissection (red arrowhead). b, A representative gross post-mortem examination of a latex-injected aorta in cross section from a *Col3a1*$^{G209S/+}$ mouse that died from a ruptured aortic dissection in the descending thoracic aorta. TL = true lumen, FL = false lumen. c, Coronal section from the aorta in (b) which demonstrates an aortic dissection in the descending thoracic aorta, with arrows pointing to elastic lamellae observed on either side of the intramural blood accumulation. TL = true lumen, FL = false lumen, EH = extravascular hemorrhage, scale bar = 100 μm.
d, e, Higher power views showing the margins of dissection in the descending thoracic aorta, arrows point to elastic lamellae observed on either side of the intramural blood accumulation, TL = true lumen, FL = false lumen, EH = extravascular hemorrhage, scale bar = 50 μm

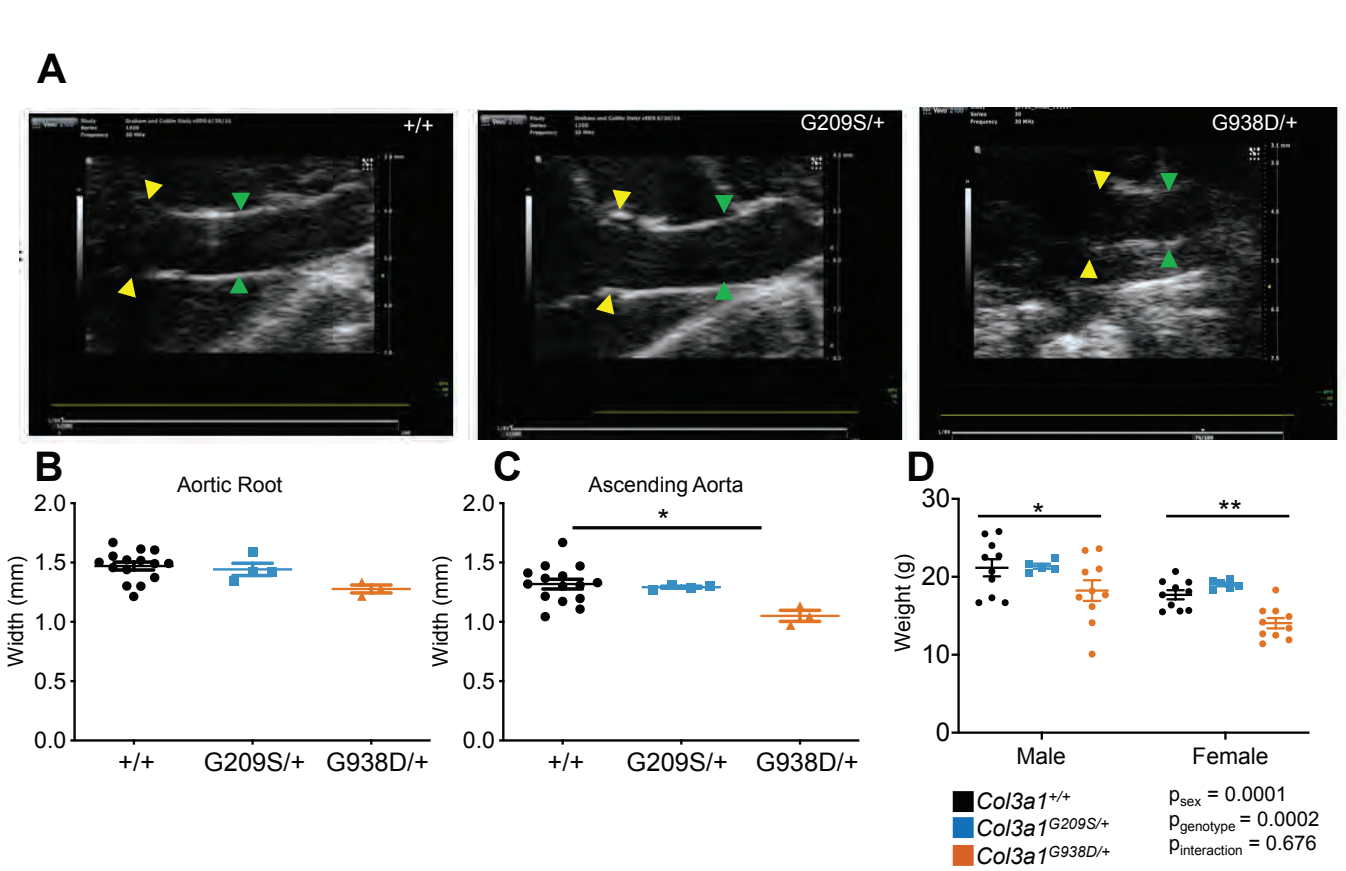

Supplementary Figure 2. vEDS mice do not have ascending aortic aneurysm.
a, Echocardiographic images of the root and ascending aorta in wild-type and vEDS mice. Yellow arrowheads point to the root and green arrowheads point to the ascending aorta. b, Measurement of aortic root diameter. Error bars show mean ± s.e. No significant differences were found using one-way ANOVA (p=0.0573, F = 3.337). c, Measurement of ascending aortic diameter. Error bars show mean ± s.e. Asterisks signify significant differences using one-way ANOVA (*p<0.05, F = 4.669) d, Weights of a cohort of male and female vEDS mice at 60 days of age. Error bars show mean ± s.e. Asterisks signify significant differences using two-way ANOVA (***p<0.001; DF = 2, F = 0.3943 interaction; DF = 1, F = 17.18 sex; DF = 2, F = 10.42 genotype)

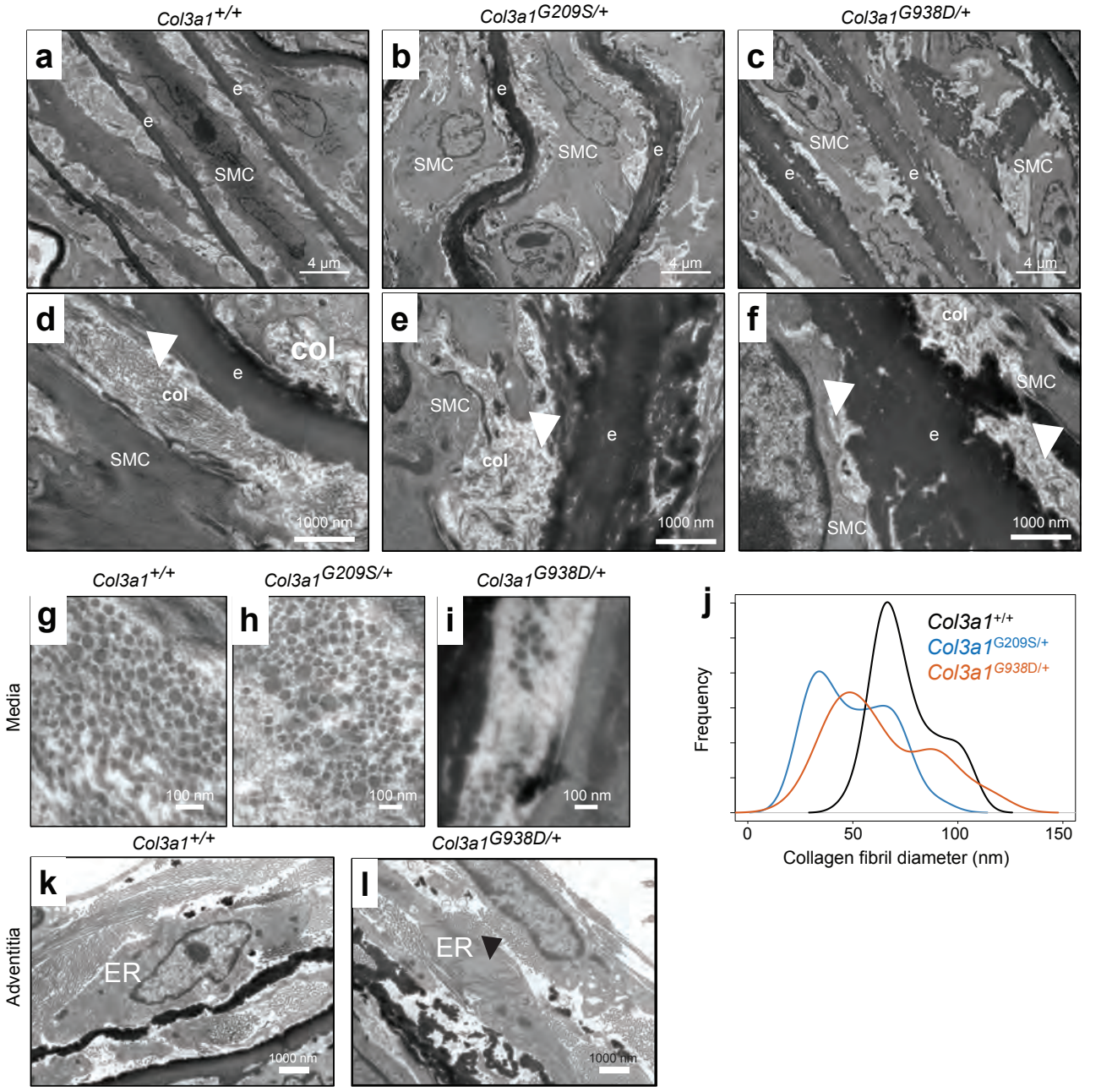

Supplementary Figure 3. vEDS aortas have abnormal extracellular matrix architecture.
a-c, electron microscopy images of the proximal descending aorta in wild-type and vEDS mice. SMC = vascular smooth muscle cell, e = elastin, col = collagen fibril. d-f, increased magnification of elastin-collagen-vascular smooth muscle cell interface in *Col3a1*$^{+/+}$, *Col3a1*$^{G209S/+}$, and *Col3a1*$^{G938D/+}$ aortas. White arrowheads indicate paucity of collagen. g-i electron microscopy images of collagen cross fiber diameter in *Col3a1*$^{+/+}$, *Col3a1*$^{G209S/+}$, and *Col3a1*$^{G938D/+}$ aortas. j, density plot demonstrating the distribution of collagen cross fiber diameters for *Col3a1*$^{+/+}$, *Col3a1*$^{G209S/+}$, and *Col3a1*$^{G938D/+}$ aortas. k,l electron microscopy images of adventitial fibroblasts in *Col3a1*$^{+/+}$, *Col3a1*$^{G209S/+}$, and *Col3a1*$^{G938D/+}$ aortas. ER = endoplasmic reticulum. Black arrowhead indicates distended ER.

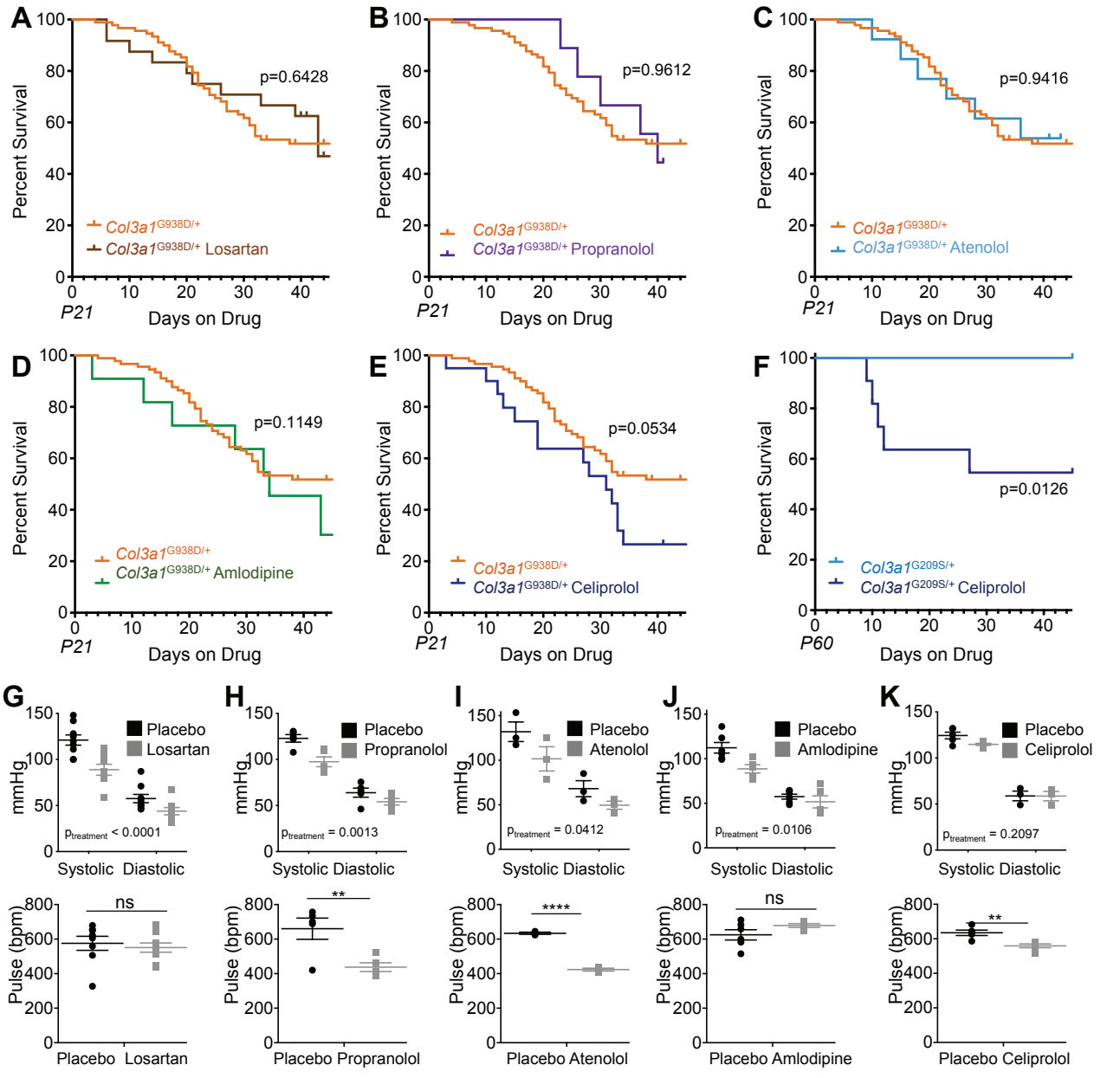

Supplementary Figure 4. Supplementary Figure 4. Losartan, propranolol, atenolol, amlodipine, and celiprolol do not rescue death from aortic rupture.

a, Kaplan-Meier survival curve comparing *Col3a1*$^{G938D/+}$ (n=93) to *Col3a1*$^{G938D/+}$ (n=24) mice receiving losartan. b, Kaplan-Meier survival curve comparing *Col3a1*$^{G938D/+}$ (n=93) to *Col3a1*$^{G938D/+}$ (n=9) mice receiving propranolol. c, Kaplan-Meier survival curve comparing *Col3a1*$^{G938D/+}$(n=93) to *Col3a1*$^{G938D/+}$ (n=13) mice receiving atenolol. d, Kaplan-Meier survival curve comparing *Col3a1*$^{G938D/+}$ (n=93) to *Col3a1*$^{G938D/+}$ (n=11) mice receiving amlodipine. e, Kaplan-Meier survival curve comparing *Col3a1*$^{G938D/+}$ (n=93) to *Col3a1*$^{G938D/+}$ (n=18) mice receiving celiprolol. f, Kaplan-Meier survival curve comparing *Col3a1*$^{G209S/+}$(n=12) to *Col3a1*$^{G209S/+}$ (n=11) mice receiving celiprolol. g, blood pressure measurements for mice on losartan. Error bars show mean ± s.e. Asterisks signify significant differences between treatment groups (pressure: DF = 1, F=20.39, pulse: t=0.5155) h, blood pressure measurements for mice on propranolol. Error bars show mean ± s.e. Asterisks signify significant differences between treatment groups (pressure: DF = 1, F =15.26, Mann-Whitney test for pulse rate, **p<0.01). i, blood pressure measurements for mice on atenolol. Error bars show mean ± s.e. Asterisks signify significant differences between treatment groups (pressure: DF=1, F=5.90, pulse: ****p<0.0001, t=20.12). j, blood pressure measurements for mice on amlodipine. Error bars show mean ± s.e. Asterisks signify significant differences between treatment groups (pressure: DF=1, F=8.134, pulse: p=0.1511, t=1.569). k, blood pressure measurements for mice on celiprolol. Error bars show mean ± s.e. Asterisks signify significant differences between treatment groups (pressure: DF=1, F=272.8, pulse: **p<0.01, t=3.959). For all survival curves, significant differences were calculated using Log-Rank (Mantel-Cox) analysis and a universal control group with N= 93 across all drug tests that started at P21. FDR-adjusted p-values are presented in Supplementary Table 3. For all blood pressure measurements, significant differences between treatment groups were determined using two-way ANOVA and a single p-value for treatment effect on both systolic and diastolic pressure is reported. For all pulse measurements, significant differences between treatment groups were determined using Student's t-test unless otherwise noted. P21 = post-natal day 21; P60 = post-natal day 60

Supplemental Figure 5. Location of the aortic section in the proximal descending thoracic aorta sent for bulk RNA sequencing.

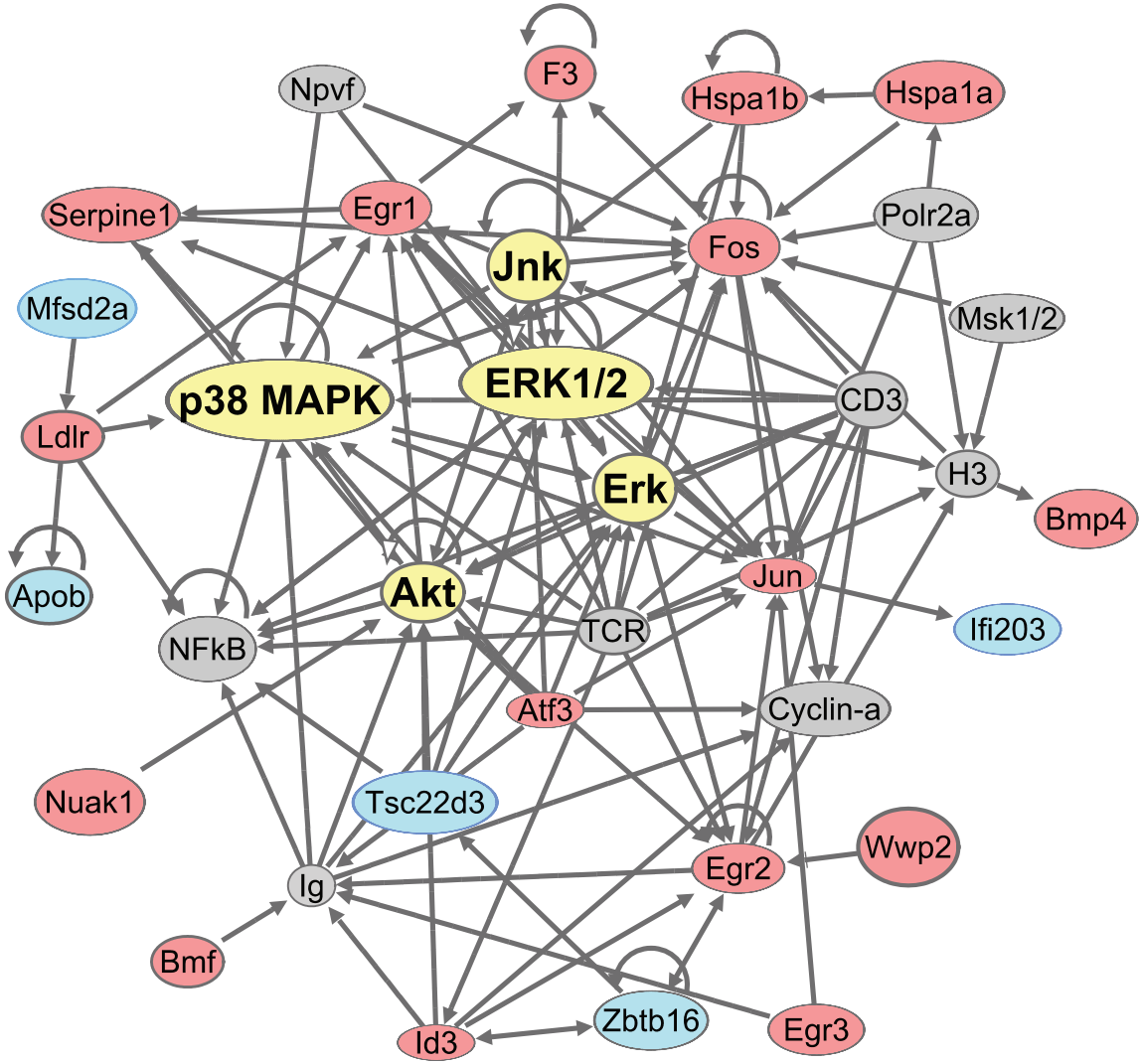

Supplementary Figure 6. Pathway analysis (Ingenuity) based on the differentially expressed genes identified by bulk RNAseq. Genes in red are upregulated and genes in blue are downregulated.

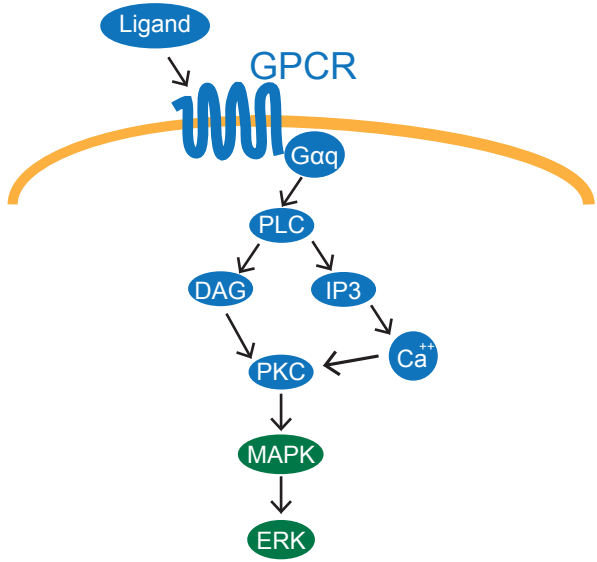

Supplementary Figure 7. Diagram illustrating proposed signaling pathway based on transcriptome profiling.

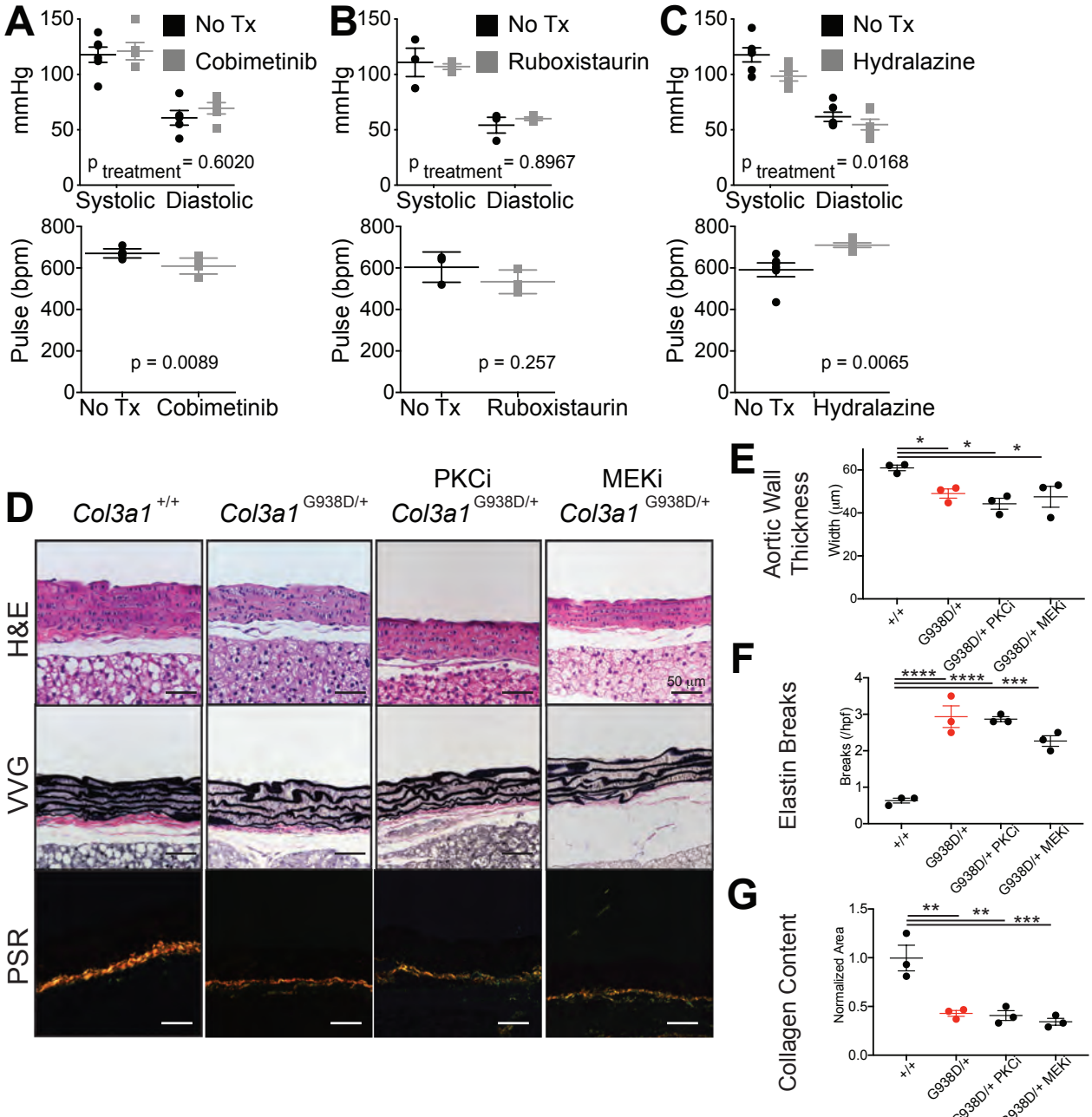

Supplementary Figure 8. Cobimetinib and Ruboxistaurin do not lower blood pressure or affect aortic wall architecture. a, blood pressure measurements for mice on cobimetinib. Error bars show mean ± s.e. Differences between treatment groups were calculated two-way ANOVA for blood pressure and Student's t-test for pulse rate (DF=1, F=0.7523, T=3.325). b, blood pressure measurements for mice on ruboxistaurin. Error bars show mean ± s.e. Differences between treatment groups were calculated using two-way ANOVA for blood pressure and Student's t-test for pulse rate (DF = 1, F=0.0179, T=2.488). c, blood pressure measurements for mice on hydralazine. Error bars show mean ± s.e. Differences between treatment groups were calculated using two-way ANOVA for blood pressure and Student's t-test for pulse rate (DF = 1, F=6.810, T=3.421). d, Histological staining (H&E = Hematoxylin & Eosin, VVG = Verhoeff Van Gieson, and PSR = Picrosirius Red) of wild type and vEDS aortic cross sections treated with ruboxistaurin (PKCi) or cobimetinib (MEKi). Scale bar = 50 µm. e, Quantification of aortic wall thickness in aortic cross sections. Error bars show mean ± s.e. Asterisks signify significant differences using one-way ANOVA with Dunnett's multiple comparisons post-hoc test (*p<0.05, DF = 3, F=5.839). f, Quantification of elastin breaks in aortic cross sections. Error bars show mean ± s.e. Asterisks signify significant differences using one-way ANOVA with Dunn's multiple comparisons post-hoc test (***p<0.001, ****p<0.0001, DF = 3, F=38.93). g, Quantification of collagen content in aortic cross sections, as measured by normalized PSR intensity. Error bars show mean ± s.e. Asterisks signify significant differences using one-way ANOVA with Dunnett's multiple comparisons post-hoc test (**p<0.01, ***p<0.001, DF = 3, F=16.91)

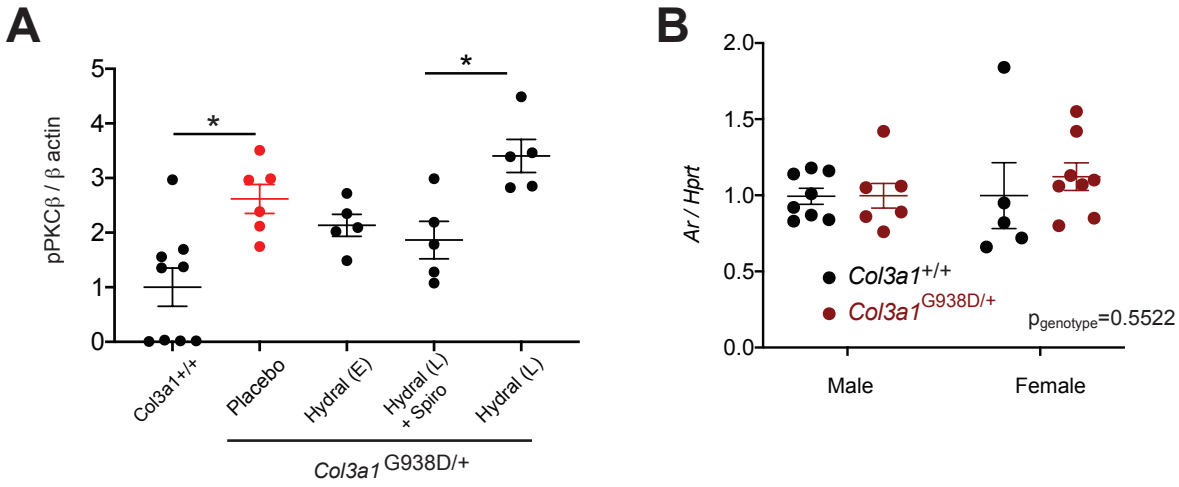

Supplementary Figure 9. Androgen signaling cross talks with PLC/IP3/PKC/ERK pathway.
a, quantification of pPKCβ levels normalized to β-actin loading control for aortas for *Col3a1*$^{+/+}$ (n=9), *Col3a1*$^{G938D/+}$ (n=6), *Col3a1*$^{G938D/+}$ mice on hydralazine sampled at age P40 (Hydral (E), n=5), *Col3a1*$^{G938D/+}$ mice on hydralazine and spironolactone sampled at age P70 (Hydral (L)+Spiro, n=5), and *Col3a1*$^{G938D/+}$ on hydralazine sampled at age P70 (Hydral (L), n=5) proximal descending aortas. Error bars show mean ± s.e. Asterisks signify significant differences using one-way ANOVA with Dunnett's multiple comparisons post-hoc test (**p<0.01, *p<0.05, DF = 4, F = 8.349). b, qPCR analysis of *Ar* normalized to *Hprt* in the proximal descending aorta comparing wild-type to *Col3a1*$^{G938D/+}$ for both male and female. Error bars show mean±s.e. Significant differences were determined using two-way ANOVA (DF = 1, F = 0.3635)

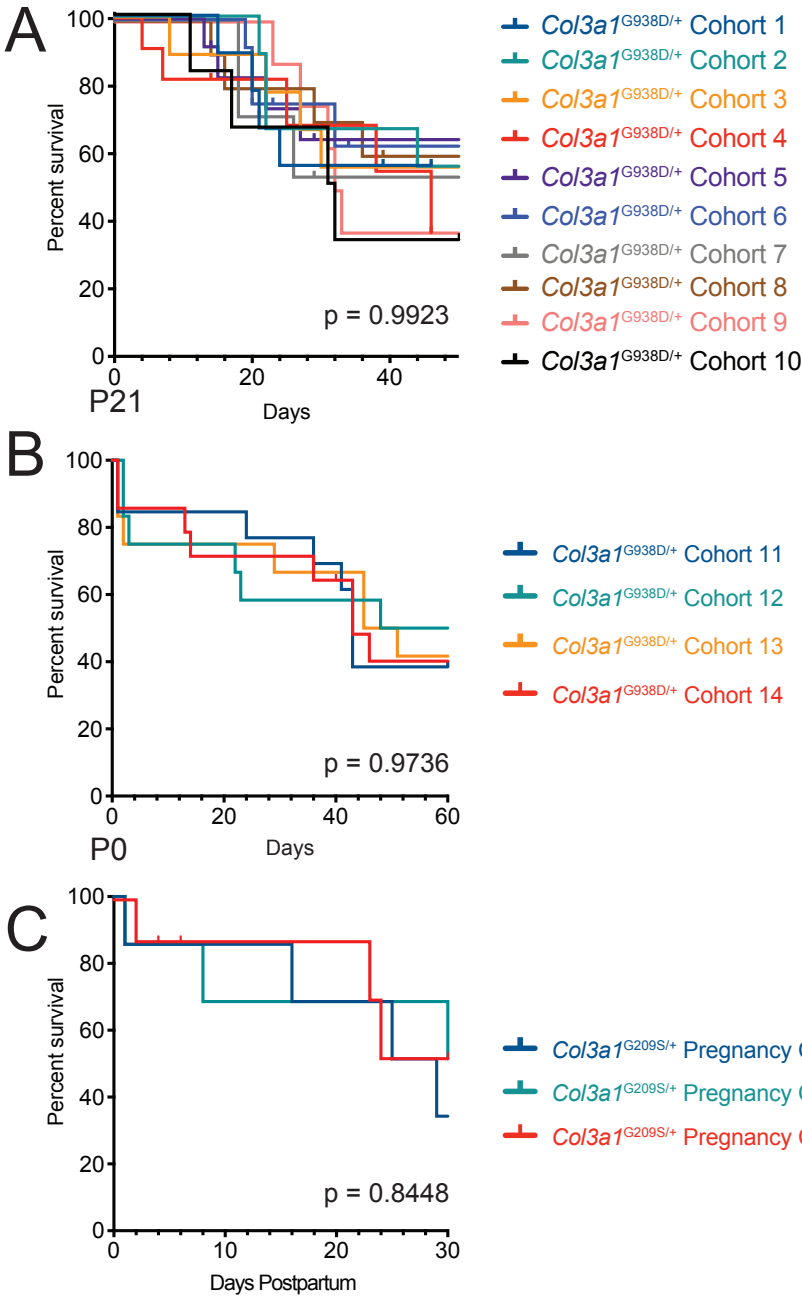

Supplementary Figure 10. Independent cohorts of untreated *Col3a1*$^{G938D/+}$ mice perform consistently over time. The p-value represents a test of whether any group differences occurred using Log-rank (Mantel-Cox) analysis. a, Control cohorts followed from P21; cohort 1: n=9, cohort 2: n=9, cohort 3: n=9, cohort 4: n=11, cohort 5: n=12, cohort 6: n=12, cohort 7: n=7, cohort 8: n=10, cohort 9: n=8, cohort 10: n=6. b, Control cohorts followed from P0; cohort 11: n=13, cohort 12: n=12, cohort 13: n=12, cohort 14: n=14. P21 = post-natal day 21; P0 = post-natal day 0. c, Control cohorts followed postpartum; cohort 1: n=7; cohort 2: n=7; cohort 3, n=8.

Tables

Supplementary Table 1. List of primers and oligonucleotide sequences.

Col3a1 G209S Forward Primer	TTTACATTCCAGGGTCCACCAG
Col3a1 G209S Reverse Primer	GTCAGGAATCTCTAAAGTTCACCTC
Col3a1 G938D Forward Primer	TCCTGGTCCTCCTGGCAATA
Col3a1 G938D Reverse Primer	TCAGATGCAAGGTGACTATGCT
gRNA 1 for Exon 7	CCTGGTGAACCTGGTCAAGC
gRNA 2 for Exon 7	CCAGGGGGACCTTGGTATC
gRNA 1 for Exon 39	AGTGGTGCTCCTGGCAAGGA
gRNA 2 for Exon 39	ACAGCAATAGCTCTCACCGG
HDR Template for Exon 7	TATATTTACACTATTCTTCTATTTTAGGGTTCTCCTGG ATACCAAGGTCCCCCTGGTGAACCTGGTCAAGCTTC TCCAGCAGTAAGTAACACTTGAGAATTGCTAAACACA TTG
HDR Template for Exon 39 (1)	GGCAAGGAAAGCAAAAAGACCCTTTTCTGCCATGTTA AAATTTAAATTATTTGCAGGGTAATCCAGGGCCCCCA GGACCCAGTGGTGCTCCTGGCAAGGACGGCCCTCC AGGTCCTGCAGGCAACAGTGGTTCTCCTGGCAACCC TGGAATAGCTGGACCAAAAGGTGATGCTGGACAGCC TGGAGAGAAGGGGCCACCTGGTGCTCAG(G/A)TCCT CCGGTGAGAGCTATTGCTGTTTTGTTGGTAGACTGC ATATTCTGATAACAAACATAATAAGGGAGCTAGGATT CTGTAGCCATAGGCTGATTCTTT
HDR Template for Exon 39 (2)	TCCTGCAGGCAACAGTGGTTCTCCTGGCAACCCTGG AATAGCTGGACCAAAAGGTGATGCTGGACAGCCTGG AGAGAAGGGGCCACCTGGTGCTCAG(G/A)TCCTCCG GTGAGAGCTATTGCTGTTTTGTTGGTAGACTGCATAT TCTGATAACAAACATAATAAGGGAGCTAGGATTCTGT AGCCATAGGCTGATTCTTTC

Supplementary Table 2. Number of male and female mice utilized in each drug trial and survival differences based on sex.

	p-value between Male and Female survival curves	Adjusted p-value (FDR)	# Male	# Female
Untreated (starting at P0)	0.7893	0.9999	27	24
Untreated (starting at P21)	0.3496	0.6554	41	52
Losartan	0.3529	0.6554	9	15
Propranolol	0.0341	0.2217	4	5
Celiprolol	0.2978	0.6554	8	10
Atenolol	0.5773	0.8338	7	6
Amlodipine	0.0871	0.3774	6	5
Ruboxistaurin	0.2568	0.6554	7	9
Cobimetinib	0.4795	0.7792	10	10
Hydralazine	0.0005	0.0065	18	23
Hydralazine + Spironolactone	0.9999	0.9999	6	10
Bicalutamide	0.9677	0.9999	12	8
Celiprolol (G209S)	0.9268	0.9999	4	7

Supplementary Table 3. FDR-adjusted p-values for survival trials.

	Unadjusted p-value	Adjusted p-value (FDR)
Losartan	0.6428	0.8264
Propranolol	0.9612	0.9612
Celiprolol	0.0534	0.0961
Atenolol	0.9416	0.9612
Amlodipine	0.1149	0.1723
Ruboxistaurin	0.0057	0.0171
Cobimetinib	0.0054	0.0171
Hydralazine + Spironolactone	<0.0001	0.0001
Bicalutamide	0.0222	0.0500
Hydralazine (Females)	0.0005	0.0010
Hydralazine + Bicalutamide (Females)	0.0385	0.0386
Hydralazine (Males)	0.1478	0.1478
Hydralazine + Bicalutamide (Males)	0.0001	0.0002
Pregnancy	0.0001	0.0006
Pregnancy + Pups Removed	0.0021	0.0031
Pregnancy + OTA	0.0314	0.0376
Pregnancy + Trametinib	0.0013	0.0026
Pregnancy + Hydralazine	0.0003	0.0009
Pregnancy + Propranolol	0.8838	0.8838

Supplementary Table 4. Assessment for influence of drugs on the survival of wild-type mice

Starting at P21	n	Unadjusted p-value	Adjusted p-value (FDR)
Untreated	129	N/A	N/A
Losartan	23	0.6576	0.7768
Propranolol	9	0.7768	0.7768
Celiprolol	11	0.7651	0.7768
Atenolol	15	0.7144	0.7768
Amlodipine	19	0.1283	0.7768
Ruboxistaurin	18	0.6885	0.7768
Cobimetinib	11	0.7540	0.7768
Hydralazine + Spironolactone	16	0.7055	0.7768
Bicalutamide	32	0.5930	0.7768

Starting at P0	n	Unadjusted p-value	Adjusted p-value (FDR)
Untreated	78	N/A	N/A
Hydralazine	48	0.2369	N/A